Chapter

A New Computerized Boundary Element Model for Three-Temperature Nonlinear Generalized Thermoelastic Stresses in Anisotropic Circular Cylindrical Plate Structures

Mohamed Abdelsabour Fahmy

Abstract

In this chapter, we propose a new theory called nonlinear generalized thermoelasticity involving three temperatures. Because of strong nonlinearity of the proposed theory, therefore, it is much more difficult to develop analytical solution for solving problems related with the proposed theory. So, we propose a new computerized boundary element model for the solution of such problems and obtaining the three-temperature nonlinear generalized thermoelastic stresses in anisotropic circular cylindrical plate structures problems which are related with the proposed theory, where we used two-dimensional three temperature nonlinear radiative heat conduction equations coupled with electron, ion and phonon temperatures. The numerical results of the current study show the temperatures effects on the thermal stresses. Also, these numerical results demonstrate the validity and accuracy of our proposed model.

Keywords: boundary element model, three-temperature radiative heat conduction, nonlinear generalized thermoelasticity, thermal stresses, anisotropic circular cylindrical plate structures

1. Introduction

The spiral formed tube which has been used in water transmission pipelines [1, 2] is the most common structural application of a cylindrical shell. Spiral formed pipes were initially constructed by riveting together appropriately bent plates [3] until advances in welding technology allowed for efficient tandem arc welding [1]. Recently, increasing attention has been devoted to the study of spiral welded tubes due to its many applications in water, gas and oil pipelines under both low and high pressure [4] as well as for foundation piles and primary load-bearing members in Combi-walls [5]. Spiral welded tubes provide certain benefits over traditional longitudinal and butt-welded tubes. In particular, continuous or very long tubular members may be constructed efficiently from compact coils of metal strip, eliminating the need for costly transport of long tubular members. The coil material is usually manufactured to very tight tolerances which results in a tube with consistent wall thickness [6]. Further, they exhibit a superior fatigue performance compared to longitudinal seam welded tubes [7]. They also exhibit a comparable resistance to crack growth propagation in ductile materials [8]. However, spiral welded tubes are not suitable for offshore and deep-water applications, because their diameter and wall thickness are limited to nearly 3 m and 30 mm, respectively [9] which generally makes them unsuitable for offshore and deep-water applications [10].

In recent years, great attention has been directed towards the study of generalized thermoelastic interactions in anisotropic thermoelastic models due to its many applications in physics, geophysics, astronautics, aeronautics, earthquake engineering, military technologies, plasma, robotics, mining engineering, accelerators, nuclear reactors, nuclear plants, soil dynamics, automobile industries, high-energy particle accelerators and other science and engineering applications. The main notion of photons, which are particles of light energy, has been introduced by Albert Einstein in 1905. It is difficult to interpret why temperature depends on the specific heat of the crystalline solids. So, the original notion of phonons, which are particles of heat, has also introduced by Albert Einstein in 1907 to explain this phenomenon. Our three-temperature study is essential for a wide range of low-temperature applications, such as pool and basin heating, unglazed and uninsulated flat-plate organic collectors, cold storage warehouses, outdoor applications in extreme low temperatures, cryogenic gas processing plants and frozen food processing facilities. Also, our three-temperature study is very important high temperature applications such as turbine blades, piston engine valves, turbo charger components, microwave devices, laser diodes, RF power amplifiers, tubes of steam power plant, recuperators in the metallurgical and glass industries. The proposed boundary element method (BEM) can be easily implemented for solving nonlinear generalized thermoelasticity problems. Through the present paper, the three-temperature concept introduced for the first time in the field of nonlinear generalized thermoelasticity. Duhamel [11] and Neumann [12] developed the classical thermo-elasticity (CTE) theory and obtained the strain-temperature gradients equations in an elastic body, but their theory has the following two shortcomings: First, the heat conduction equation is predicting infinite speeds of propagation. Second, the heat conduction equation does not contain elastic terms. Biot [13] developed the classical coupled thermo-elasticity (CCTE) theory to overcome the first shortcoming in CTE. Then, several generalized theories based on a modified Fourier's law predict finite propagation speed of thermal waves such as extended thermo-elasticity (ETE) theory of Lord and Shulman (L-S) [14], temperature-rate-dependent thermo-elasticity (TRDTE) theory of Green and Lindsay (G-L) [15] and three linear generalized thermoelasticity models of Green and Naghdi (G-N) [16, 17], where Type I discusses the heat conduction theory based on Fourier's law, type II describes the thermoelasticity theory without energy dissipation (TEWOED), and type III discusses the thermoelasticity theory with energy dissipation (TEWED). Due to the computational difficulties, inherent in solving nonlinear generalized thermoelastic problems [18], for such problems, it is very difficult to obtain the analytical solution in a general case. Instead of analytical methods, many numerical methods were developed for solving such problems approximately including the finite difference method (FDM) [19, 20], discontinuous Galerkin method (DGM) [21], finite element method (FEM) [22, 23] and boundary element method (BEM) [24–26]. The boundary element method (BEM) has been performed successfully for solving various engineering, scientific and mathematical applications due to its simplicity, efficiency, and ease of implementation [27–46].

The main aim of the present chapter is to propose a new theory called nonlinear generalized thermoelasticity involving three-temperature. A new boundary element model was proposed for solving nonlinear generalized thermoelastic problems in anisotropic circular cylindrical plate structures which are associated with the proposed theory, where we used two-dimensional three-temperature (2D-3T) nonlinear time-dependent radiative heat conduction equations coupled with electron, ion and photon temperatures in the formulation of such problems. The numerical results are presented graphically to show the effects of electron, ion and photon temperatures on the thermal stress components. The validity and accuracy of our proposed BEM model were confirmed by comparing our BEM obtained results with the corresponding results of finite element method (FEM).

A brief summary of the chapter is as follows: Section 1 outlines the background and provides the readers with the necessary information to books and articles for a better understanding of mechanical behaviour of anisotropic circular cylindrical plate structures and their applications. Section 2 describes the formulation of the new theory and its related problems. Section 3 discusses the implementation of the new BEM for solving the three-temperature heat conduction equations, to obtain the temperature fields. Section 4 studies the development of new BEM and its implementation for solving the equilibrium equation based on the three-temperature fields. Section 5 presents the new numerical results that describe the temperatures effects on the thermal stresses generated in anisotropic circular cylindrical plate structures.

2. Formulation of the problem

We consider a cylindrical coordinate system (r, θ, z) for the circular cylindrical plate structure (**Figure 1**) within the region R which bounded by boundary S. Pressure distribution over the structure's entire surface has been shown in **Figure 2**. Geometry of meridional cross section of the considered structure has been shown in **Figure 3**, where $d\theta = \frac{1}{r}$.

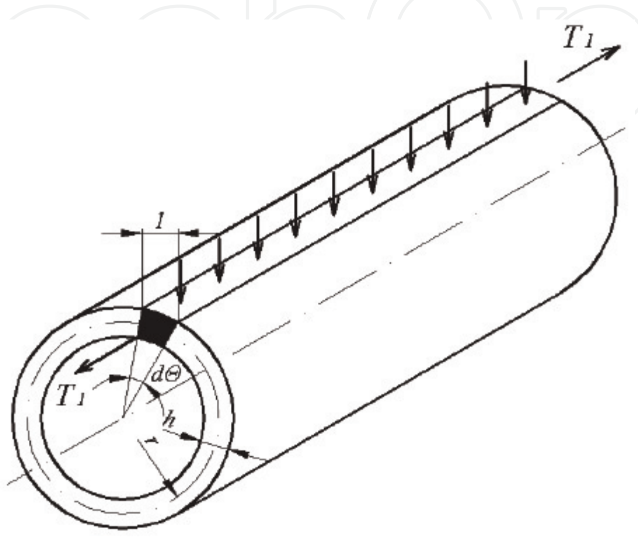

Figure 1.
Geometry of circular cylindrical plate structure.

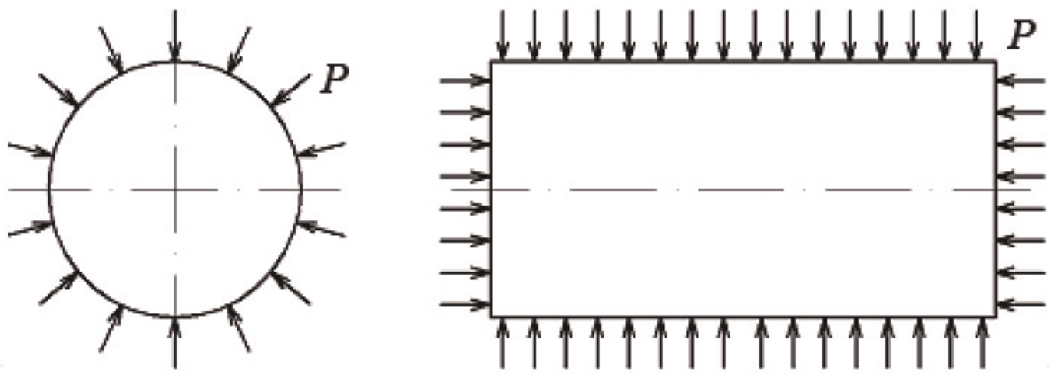

Figure 2.
Pressure distribution over the structure's entire surface.

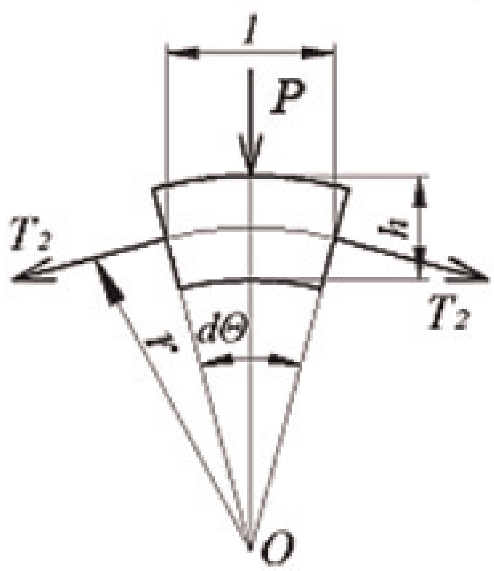

Figure 3.
Geometry of meridional cross section of considered structure.

The equilibrium equations for anisotropic plate structures can be written as follows

$$\sigma_{pj,j} = 0 \tag{1}$$

where

$$\sigma_{pj} = C_{pjkl} u_{k,l} - \beta_{pj} T_\alpha(r, \tau) \tag{2}$$

Three radiative heat conduction equations coupled with electron, ion and phonon temperatures can be written as follows

$$c_e \frac{\partial T_e(r,\tau)}{\partial \tau} - \frac{1}{\rho} \nabla[\mathbb{K}_e \nabla T_e(r,\tau)] = -\mathbb{W}_{ei}(T_e - T_i) - \mathbb{W}_{ep}\left(T_e - T_p\right) \tag{3}$$

$$c_i \frac{\partial T_i(r,\tau)}{\partial \tau} - \frac{1}{\rho} \nabla[\mathbb{K}_i \nabla T_i(r,\tau)] = \mathbb{W}_{ei}(T_e - T_i) \tag{4}$$

$$\frac{4}{\rho} c_p T_p^3 \frac{\partial T_p(r,\tau)}{\partial \tau} - \frac{1}{\rho} \nabla\left[\mathbb{K}_p \nabla T_p(r,\tau)\right] = \mathbb{W}_{ep}\left(T_e - T_p\right) \tag{5}$$

where $\left(T_e, T_i, T_p\right)$, $\left(c_e, c_i, c_p\right)$ and $\left(\mathbb{K}_e, \mathbb{K}_i, \mathbb{K}_p\right)$ are respectively temperatures, specific heat capacities and conductive coefficients of electron, ion and phonon.

The total temperature

$$T = T_e + T_i + T_p \tag{6}$$

3. BEM solution for three-temperature field

The nonlinear time-dependent two dimensions three temperature (2D-3T) radiative heat conduction Eqs. (3)–(5) coupled by electron, ion and phonon temperatures can be written as

$$\nabla\left[\left(\delta_{1j}\mathbb{K}_\alpha + \delta_{2j}\mathbb{K}_\alpha^*\right)\nabla T_\alpha(r,\tau)\right] - \overline{\mathbb{W}}(r,\tau) = c_\alpha \rho \delta_1 \delta_{1j}\frac{\partial T_\alpha(r,\tau)}{\partial \tau} \tag{7}$$

where

$$\overline{\mathbb{W}}(r,\tau) = \begin{cases} \rho\,\mathbb{W}_{ei}(T_e - T_i) + \rho\,\mathbb{W}_{er}\left(T_e - T_p\right) + \overline{\overline{\mathbb{W}}}, \alpha = e, \delta_1 = 1 \\ -\rho\mathbb{W}_{ei}(T_e - T_i) + \overline{\overline{\mathbb{W}}}, \quad \alpha = i, \delta_1 = 1 \\ -\rho\mathbb{W}_{er}\left(T_e - T_p\right) + \overline{\overline{\mathbb{W}}}, \quad \alpha = p, \delta_1 = \dfrac{4}{\rho}T_p^3 \end{cases} \tag{8}$$

$$\overline{\overline{\mathbb{W}}}(r,\tau) = -\delta_{2j}\mathbb{K}_\alpha \dot{T}_{\alpha,ab} + \beta_{ab}T_{\alpha 0}\left[\text{Å}\delta_{1j}\dot{u}_{a,b} + \left(\tau_0 + \delta_{2j}\right)\ddot{u}_{a,b}\right] + \rho c_\alpha\left[\left(\tau_0 + \delta_{1j}\tau_2 + \delta_{2j}\right)\ddot{T}_\alpha\right] - \frac{T_{\alpha,a}}{r}, \quad \frac{T_{\alpha,a}}{r} = T_{\alpha,aa} \tag{9}$$

$$\mathbb{W}_{ei} = \rho\mathbb{A}_{ei}T_e^{-2/3}, \mathbb{W}_{er} = \rho\mathbb{A}_{er}T_e^{-1/2}, \mathbb{K}_\alpha = \mathbb{A}_\alpha T_\alpha^{5/2}, \alpha = e, i, \mathbb{K}_p = \mathbb{A}_p T_p^{3+\mathbb{B}} \tag{10}$$

The total energy can be written as follows

$$P = P_e + P_i + P_p, P_e = c_e T_e, P_i = c_i T_i, P_p = \frac{1}{\rho}c_p T_p^4 \tag{11}$$

By applying the following conditions

$$T_\alpha(x,y,0) = T_\alpha^0(x,y) = g_1(x,\tau) \tag{12}$$

$$\mathbb{K}_\alpha \frac{\partial T_\alpha}{\partial n}\bigg|_{\Gamma_1} = 0, \alpha = e, i, T_r|_{\Gamma_1} = g_2(x,\tau) \tag{13}$$

$$\mathbb{K}_\alpha \frac{\partial T_\alpha}{\partial n}\bigg|_{\Gamma_2} = 0, \alpha = e, i, p \tag{14}$$

By using the fundamental solution that satisfies the following Eq. [46]

$$D\nabla^2 T_\alpha + \frac{\partial T_\alpha^*}{\partial n} = -\delta\left(r - p_i\right)\delta(\tau - r) \tag{15}$$

where $D = \frac{\mathbb{K}_\alpha}{\rho c}$ and p_i are singular points.

The corresponding dual reciprocity boundary integral equation can be written as [46]

$$CT_\alpha = \frac{D}{\mathbb{K}_\alpha}\int_O^\tau\int_S\left[T_\alpha q^* - T_\alpha^* q\right]dSd\tau + \frac{D}{\mathbb{K}_\alpha}\int_O^\tau\int_R bT_\alpha^* dRd\tau + \int_R T_\alpha^i T_\alpha^*\big|_{\tau=0}dR \tag{16}$$

which can be expressed as

$$CT_{\alpha} = \int_S \left[T_{\alpha}q^* - T_{\alpha}^* q\right] dS - \int_R \frac{\mathbb{K}_{\alpha}}{D}\frac{\partial T_{\alpha}^*}{\partial \tau} T_{\alpha} dR \tag{17}$$

In order to transform the domain integral into the boundary, we assume that

$$\frac{\partial T_{\alpha}}{\partial \tau} \cong \sum_{j=1}^{N} f^j(r)^j a^j(\tau) \tag{18}$$

where $f^j(r)$ and $a^j(\tau)$ are known functions and unknown coefficients, respectively.

We assume that $\hat{T}_{\alpha}^{j}$ is a solution of

$$\nabla^2 \hat{T}_{\alpha}^{j} = f^j \tag{19}$$

Thus, from (17) we can write the following boundary integral equation

$$CT_{\alpha} = \int_S \left[T_{\alpha}q^* - T_{\alpha}^* q\right] dS + \sum_{j=1}^{N} a^j(\tau) D^{-1}\left(C\hat{T}_{\alpha}^{j} - \int_S \left[T_{\alpha}^{j} q^* - \hat{q}^j T_{\alpha}^*\right] dS\right) \tag{20}$$

where

$$\hat{q}^j = -\mathbb{K}_{\alpha}\frac{\partial \hat{T}_{\alpha}^{j}}{\partial n} \tag{21}$$

$$a^j(\tau) = \sum_{i=1}^{N} f_{ji}^{-1}\frac{\partial T(r_i, \tau)}{\partial \tau} \tag{22}$$

$$\{F\}_{ji} = f^j(r_i) \tag{23}$$

By using (20) and (22), we obtain

$$C\dot{T}_{\alpha} + HT_{\alpha} = GQ \tag{24}$$

where

$$C = -\left[H\hat{T}_{\alpha} - G\hat{Q}\right] F^{-1} D^{-1} \tag{25}$$

and

$$\left\{\hat{T}\right\}_{ij} = \hat{T}^j(x_i) \tag{26}$$

$$\left\{\hat{Q}\right\}_{ij} = \hat{q}^j(x_i) \tag{27}$$

For solving (24) numerically, the functions q, T_{α} and its derivative with time can be written as

$$q = (1-\Theta)q^m + \Theta\, q^{m+1}, 0 \leq \Theta \leq 1 \tag{28}$$

$$T_\alpha = (1-\Theta)T_\alpha^m + \theta T_\alpha^{m+1}, 0 \le \Theta = \frac{\tau - \tau^m}{\tau^{m+1} - \tau^m} \le 1 \tag{29}$$

$$\dot{T}_\alpha = \frac{dT_\alpha}{d\Theta}\frac{d\Theta}{d\tau} = \frac{T_\alpha^{m+1} - T_\alpha^m}{\tau^{m+1} - \tau^m} = \frac{T_\alpha^{m+1} - T_\alpha^m}{\Delta\tau^m} \tag{30}$$

By substituting from Eqs. (28)–(30) into Eq. (24), we obtain

$$\left(\frac{C}{\Delta\tau^m} + \Theta H\right)T_\alpha^{m+1} - \Theta G Q^{m+1} = \left(\frac{C}{\Delta\tau^m} - (1-\Theta)H\right)T_\alpha^m + (1-\Theta)GQ^m \tag{31}$$

By applying the initial and boundary conditions, we obtain

$$\mathbb{a}\mathrm{X} = \mathbb{b} \tag{32}$$

This system yields the temperature in terms of the displacement field.

4. BEM solution for displacement field

The equilibrium Eqs. (1) for anisotropic plate structures can be written as follows [47]

$$C_{ijkl}\frac{d^4 w}{dx^4} - T\frac{d^2 w}{dx^2} = p + \frac{T_1}{r} \tag{33}$$

where

$$T_2 = -\frac{pr}{2} \tag{34}$$

$$T_1 = C_{ijkl}T_2 - C_{ijkl}h\frac{w}{r} \tag{35}$$

By using (34) and (35), we can write (33) in the following form

$$C_{ijkl}\frac{d^4 w}{dx^4} + \frac{pr}{2}\frac{d^2 w}{dx^2} + \frac{C_{ijkl}h}{r^2}w = p\left(1 - \frac{C_{ijkl}}{2}\right) \tag{36}$$

where

$$\mathrm{A} = \frac{C_{ijkl}h}{r^2} \tag{37}$$

$$\mathrm{B} = p\left(1 - \frac{C_{ijkl}}{2}\right) \tag{38}$$

By using Eqs. (37) and (38), we can write (36) as follows

$$C_{ijkl}\frac{d^4 w}{dx^4} - T\frac{d^2 w}{dx^2} + \mathrm{A}w = \mathrm{B} \tag{39}$$

where

$$\beta = \frac{T_2}{2\sqrt{C_{ijkl}k}}, 0 < \beta^2 < 1 \tag{40}$$

The general solution of (39) can be obtained as

$$w(x) = C_1 ch\delta x \cos\gamma x + C_2 ch\delta x \sin\gamma x + C_3 sh\delta x \cos\gamma x + C_4 sh\delta x \sin\gamma x + w_{\text{part}} \tag{41}$$

where

$$\delta = \alpha\sqrt{1+\beta}; \gamma = \alpha\sqrt{1-\beta}; \alpha = \sqrt[4]{\frac{k}{4C_{ijkl}}}, \beta = \frac{T_2}{2\sqrt{C_{ijkl}k}} \tag{42}$$

and the particular solution can be determined as $p =$ constant as follows

$$w_{\text{part}} = \frac{pr^2}{C_{ijkl}h}\left(1 - \frac{C_{ijkl}}{2}\right) \tag{43}$$

Thus, Eq. (41) can be written as

$$w(x) = \frac{pr^2}{C_{ijkl}h}\left(1 - \frac{C_{ijkl}}{2}\right) + C_1 ch\delta x \cos\gamma x + C_4 sh\delta x \sin\gamma x \tag{44}$$

By implementing the following boundary conditions.

$$\text{at } x = \pm\frac{l}{2}\frac{dw}{dx} = 0 \tag{45}$$

$$\text{at } x = \frac{l}{2} w = \frac{2pr^2}{C_{ijkl}h}\frac{d^3w}{dx^3} \tag{46}$$

we can write the unknown C_1 and C_4 as follows

$$C_1 = -\frac{2pr^2}{C_{ijkl}h}\left(1 - \frac{C_{ijkl}}{2}\right)\frac{u_1 chu_1 \sin u_2 + u_2 shu_1 \cos u_2}{u_2 sh2u_1 + u_1 \sin 2u_2}\varepsilon_1 \tag{47}$$

$$C_4 = -\frac{2pr^2}{C_{ijkl}h}\left(1 - \frac{C_{ijkl}}{2}\right)\frac{u_2 chu_1 \sin u_2 - u_1 shu_1 \cos u_2}{u_2 sh2u_1 + u_1 \sin 2u_2}\varepsilon_1 \tag{48}$$

where

$$\varepsilon_1 = \frac{1}{1 + \frac{lh}{A}A_1(u_1, u_2)} \tag{49}$$

$$A_1(u_1, u_2) = \sqrt{1-\beta^2}\frac{ch2u_1 - \cos 2u_2}{u_2 sh2u_1 + u_1 \sin 2u_2} \tag{50}$$

$$u_1 = \frac{\delta l}{2} = u\sqrt{1+\beta}, u_2 = \frac{\gamma l}{2} = u\sqrt{1+\beta}, u = 0.6425\frac{1}{\sqrt{rh}} \tag{51}$$

If we neglected the longitudinal forces influence on the bending of the circular cylindrical shell, we can write (39) in the following form

$$C_{ijkl}w^{IV} + kw = q \tag{52}$$

Now, the approximate solution has been reduced for solving problem of bending single span beam with the following compliance

$$k_{II} = \frac{2r^2}{C_{ijkl}A} \tag{53}$$

The deflection of the considered shell in the cross section and reference section, respectively, is as follows

$$w(0) = \frac{pr^2}{C_{ijkl}h}\left(1 - \frac{v}{2}\right)\left[1 - \frac{\varnothing_1(u)}{1 + B_1}\right] \tag{54}$$

$$w\left(\frac{l}{2}\right) = \frac{pr^2}{C_{ijkl}h}\left(1 - \frac{v}{2}\right)\frac{B_1}{1 + B_1} \tag{55}$$

Also, the bending moment in the cross section and reference section, respectively, is as follows

$$M_1(0) = -\frac{pl^2}{24}\left(1 - \frac{v}{2}\right)\left[1 - \frac{\chi_1(u)}{1 + B_1}\right] \tag{56}$$

$$M_1\left(\frac{l}{2}\right) = \frac{pl^2}{12}\left(1 - \frac{v}{2}\right)\frac{\chi_2(u)}{1 + B_1} \tag{57}$$

The Cauchy model with two-bed scheme can be described as follows

$$Dv^{IY}(x) + \frac{pr}{2}v''(x) + \frac{C_{ijkl}h}{r^2}v(x) = p\left(1 - \frac{\mu}{2}\right) \tag{58}$$

$$v(0); \varphi(0) = v'(0) \tag{59}$$

$$M(0) = -Dv''(0) - Tv(0) \tag{60}$$

$$Q(0) = -Dv'''(0) - Tv'(0) \tag{61}$$

where the characteristic equation of (58) can be defined as

$$C_{ijkl}k^4 + \frac{pr}{2}k^2 + \frac{C_{ijkl}h}{r^2} = 0, k^2 = t \tag{62}$$

$$C_{ijkl}t^2 + \frac{pr}{2}t + \frac{C_{ijkl}h}{r^2} = 0 \tag{63}$$

which roots

$$k_{1,2,3,4} = \pm\sqrt{\frac{-\frac{pr}{2} \pm \sqrt{\left(\frac{pr}{2}\right)^2 - 4C_{ijkl}{}^2\frac{h}{r^2}}}{2C_{ijkl}}} \tag{64}$$

$$t_{1,2} = \frac{-\frac{pr}{2} \pm \sqrt{\left(\frac{pr}{2}\right)^2 - 4C_{ijkl}{}^2\frac{h}{r^2}}}{2C_{ijkl}} \tag{65}$$

The systems (32) and (58) can be solved by using the algorithm of Fahmy [35] to obtain the three temperatures and displacements components. Then we can compute thermal stresses distributions along radial distance r. we refer the reader to recent references [48–51] for details of boundary element technique.

5. Numerical results and discussion

The BEM that has been used in the current chapter can be applicable to a wide variety *of plate structures problems* associated with the proposed theory of three temperatures nonlinear generalized thermoelasticity. In order to evaluate temperatures effects on the thermal stresses, the numerical results are carried out and depicted graphically for electron, ion and phonon temperatures.

Figure 4 shows the distributions of the three temperatures T_e, T_i, T_p and total temperature T $\left(T = T_e + T_i + T_p\right)$ along the radial distance r. It was shown from this figure that the three temperatures are different and they may have great effects on the connected fields.

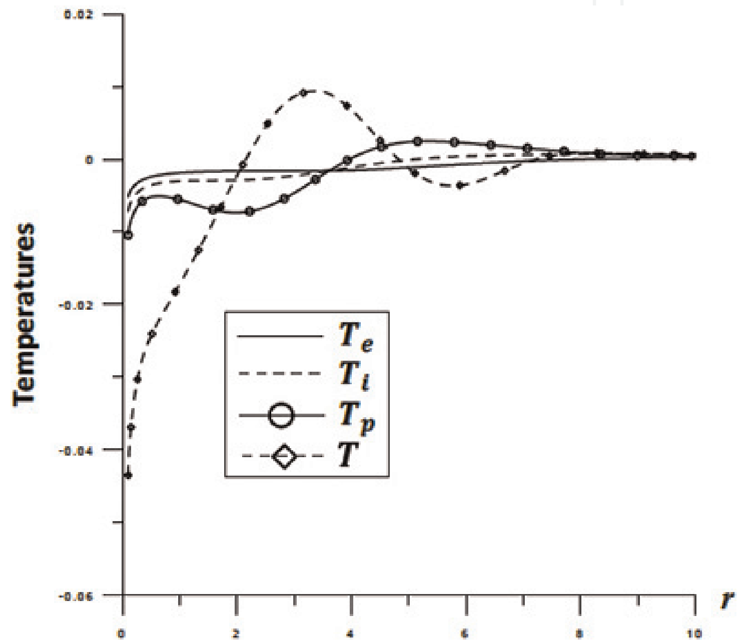

Figure 4.
Variation of the temperatures T_e, T_i, T_p and T along the radial distance r.

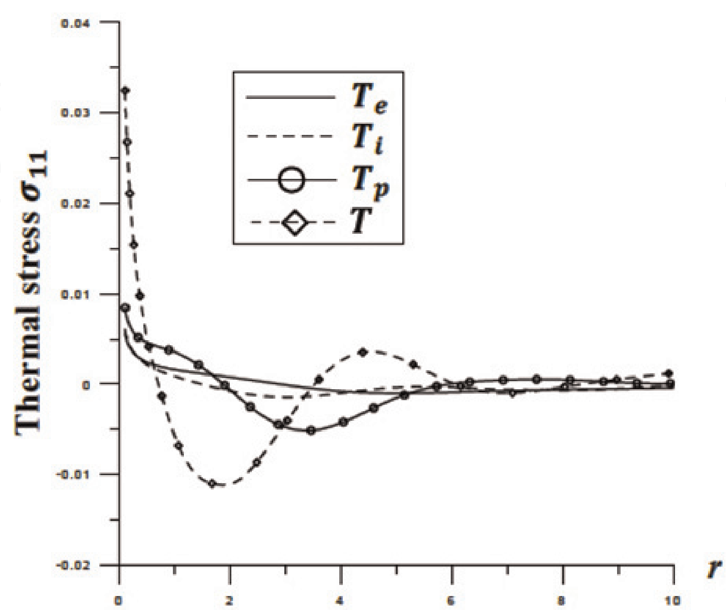

Figure 5.
Variation of the thermal stress σ_{11} with radial distance r.

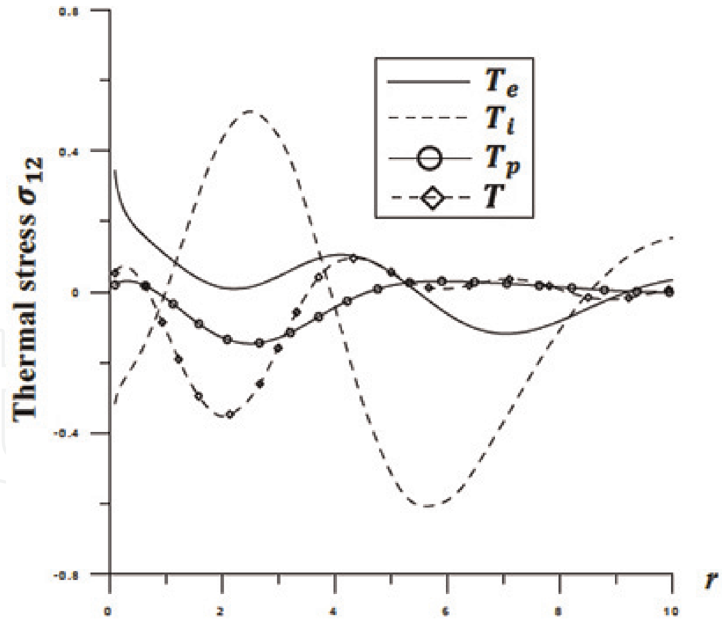

Figure 6.
Variation of the thermal stress σ_{12} with radial distance r.

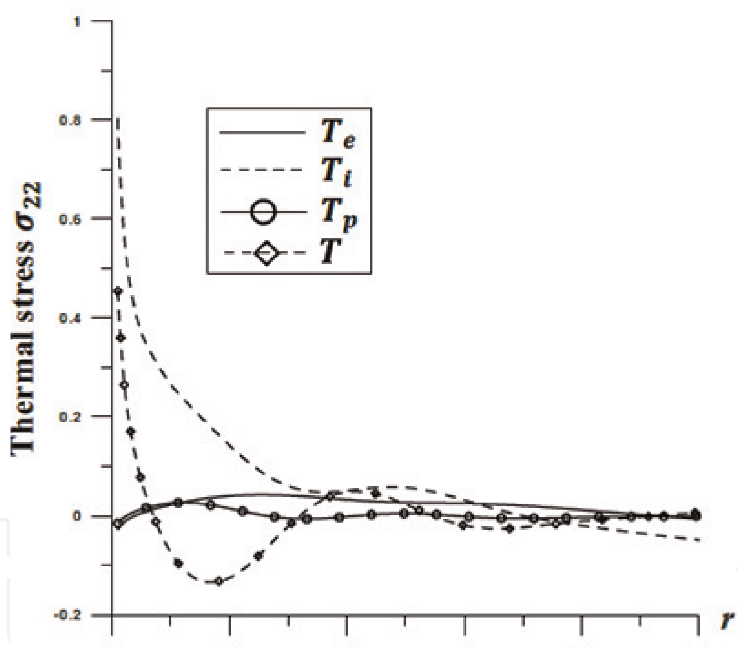

Figure 7.
Variation of the thermal stress σ_{22} with radial distance r.

Figures 5–7 show the distributions of the thermal stresses σ_{11}, σ_{12} and σ_{22} respectively, with the radial distance r for the three temperatures T_e, T_i, T_p and total temperature. It was noticed from these figures that the three temperatures have great effects on the thermal stresses.

Figure 8 shows the distributions of the thermal stresses $\sigma_{11}, \sigma_{12}, \sigma_{22}$ and total temperature T with the radial distance r for BEM results and finite element method (FEM) results of COMSOL Multiphysics software version 5.4 to demonstrate the validity and accuracy of our proposed model based on replacing heat conduction with three-temperature heat conduction.

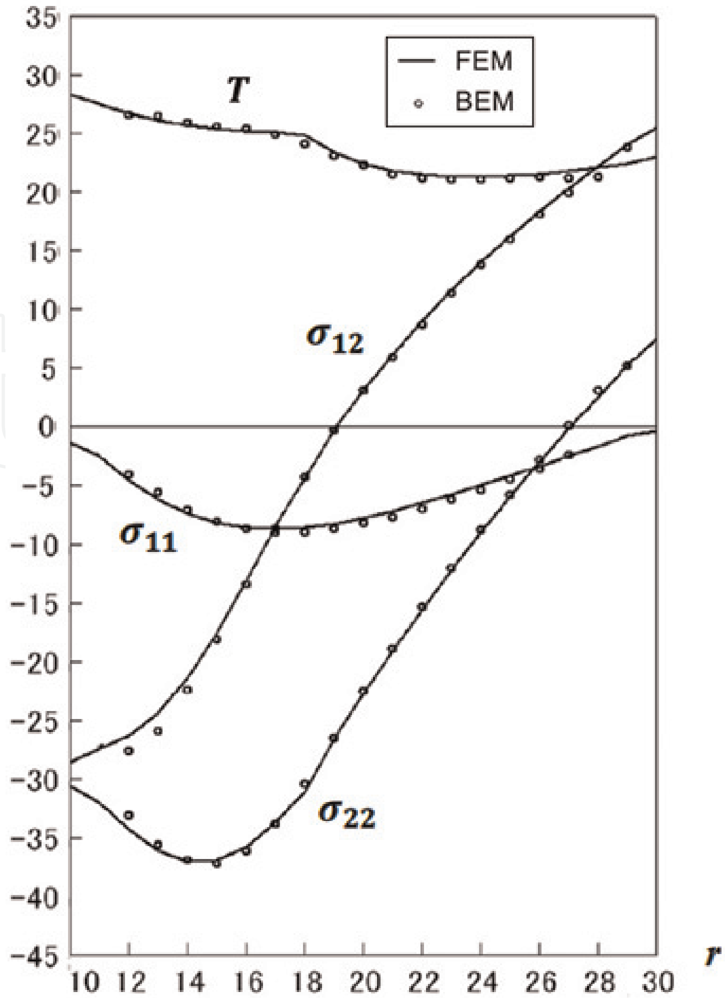

Figure 8.
Thermal stresses and total temperature variations with r.

6. Conclusion

The main objective of this chapter is to propose a new theory called nonlinear generalized thermoelasticity involving three-temperature and new BEM model for the solution of problems which are associated with the proposed nonlinear theory, where we used the three-temperature radiative heat conduction equations coupled with electron, ion and phonon temperatures to describe the thermal stresses in anisotropic circular cylindrical plate structures. It can be concluded from numerical results of our proposed model that the generalized theories of thermoelasticity can be connected with the three-temperature radiative heat conduction to describe the deformation of anisotropic circular cylindrical plate structures. The validity and accuracy of the proposed model was examined and confirmed by comparing the obtained results with those known previously. Because there are no available data to confirm the validity and accuracy of our results, we replace the three-temperature radiative heat conduction results with one-temperature heat conduction results as a special case from results of our current general model for circular cylindrical plate structures. In the special case under consideration, the results obtained with the BEM have been compared graphically with the FEM results of COMSOL Multiphysics software version 5.4. Excellent agreement is obtained between BEM results and FEM results. Understanding the behaviour of the three-temperature thermal stresses in anisotropic circular cylindrical plate structures should be a key for extending the application of these behaviors to a wide range of structures. The numerical results for our general model which is associated with our proposed theory may provide interesting information for computer scientists and engineers, geotechnical and geothermal engineers, researchers who will industrialize the thermoelastic devices using additive manufacturing and the materials designers and developers, etc.

Nomenclature

β_{ij}	stress-temperature coefficients
δ_{ij}	Kronecker delta $(i, j = 1, 2)$
ε_{ij}	strain tensor
θ	thermodynamic temperature
λ	tractions
μ_0	magnetic permeability
ϑ_0	viscoelastic relaxation time
ϖ	weights of control points
ρ	density
σ_{ij}	force stress tensor
c	specific heat capacity
C_{ijkl}	constant elastic moduli
$\mathbb{e}_{lij}$	piezoelectric tensor
F_i	mass force vector
$\mathbb{K}_\alpha$	conductive coefficients
M_1	bending moment
P	total energy of unit mass
T_α	temperature functions
u_i	displacement vector
$w(x)$	general solution
$\mathbb{W}_{ei}$	electron-ion energy coefficient
$\mathbb{W}_{ep}$	electron-photon energy coefficient

Author details

Mohamed Abdelsabour Fahmy
Faculty of Computers and Informatics, Suez Canal University, Ismailia, Egypt

*Address all correspondence to: mohamed_fahmy@ci.suez.edu.eg

References

[1] Hanada M, Takeda H, Fukushima H, Koizumi I, Noguchi Y. Development of highspeed submerged arc welding in spiral pipe mill. Transactions of the Iron and Steel Institute of Japan. 1986;**26**: 433-438

[2] Burstall T. Bulk Water Pipelines. London, United Kingdom: Thomas Telford Ltd.; 1997

[3] Hardenbergh WA. Water Supply and Purification. 2nd ed. Scranton, PA: International Textbook Company; 1945

[4] Liu H. Pipeline engineering. Florida, United States: CRC Press; 2003

[5] CUR. Handbook Quay Walls– Publication N. 211 E. Gouda, Holland: Centre for Civil Engineering Research and Codes (CUR); 2005

[6] Lancaster J. Handbook of Structural Welding: Processes, Materials and Methodsused in the Welding of Major Structures, Pipelines and Process Plants. Cambridge, United Kingdom: Woodhead Publishing; 1997

[7] Radaj D. Design and Analysis of Fatigue Resistant Welded Structures. Cambridge, United Kingdom: Woodhead Publishing; 1990

[8] Andrews RM, Pistone V. European pipeline research group studies on ductilecrack propagation in gas transmission pipelines. European Structural Integrity Society. 2002;**30**: 377-384

[9] Mittal A. Spirally Welded Steel Pipes. The Netherlands: Corporate Brochure, Projects-Europe, Foundation Solutions; 2011

[10] Gerwick BC. Construction of Marine and Offshore Structures. 3rd ed. Florida, United States: CRC Press; 2007

[11] Duhamel J. Some memoire sur les phenomenes thermo-mechanique. Journal de l'École Polytechnique. 1837; **15**:1-57

[12] Neumann F. Vorlesungen Uber die theorie der elasticitat. Brestau: Meyer; 1885

[13] Biot M. Thermoelasticity and irreversible thermo-dynamics. Journal of Applied Physics. 1956;**27**:249-253

[14] Lord HW, Shulman Y. A generalized dynamical theory of thermoelasticity. Journal of the Mechanics and Physics of Solids. 1967; **15**:299-309

[15] Green AE, Lindsay KA. Thermoelasticity. Journal of Elasticity. 1972;**2**:1-7

[16] Green AE, Naghdi PM. On undamped heat waves in an elastic solid. Journal of Thermal Stresses. 1992;**15**: 253-264

[17] Green AE, Naghdi PM. Thermoelasticity without energy dissipation. Journal of Elasticity. 1993; **31**:189-208

[18] Jafarian A, Ghaderi P, Golmankhaneh AK, Baleanu D. Analytic solution for a nonlinear problem of magneto-Thermoelasticity. Reports on Mathematical Physics. 2013;**71**:399-411. DOI: 10.1016/S0034-4877(13)60039-7

[19] Abd-El-Salam MR, Abd-Alla AM, Hosham HA. A numerical solution of magneto-thermoelastic problem in non-homogeneous isotropic cylinder by the finite-difference method. Applied Mathematical Modelling. 2007;**31**: 1662-1670. DOI: 10.1016/j.apm.2006.05.009

[20] Abd-Alla AM, El-Naggar AM, Fahmy MA. Magneto-thermoelastic problem in non-homogeneous isotropic cylinder. Heat and Mass Transfer. 2003; **39**:625-629

[21] Hu Q, Zhao L. Domain decomposition preconditioners for the system generated by discontinuous Galerkin discretization of 2D-3T heat conduction equations. Communications in Computational Physics. 2017;**22**: 1069-1100

[22] Abbas IA, Abd-alla AN, Othman MIA. Generalized magneto-thermoelasticity in a fiber-reinforced anisotropic half-space. International Journal of Thermophysics. 2011;**32**: 1071-1085. DOI: 10.1007/s10765-011-0957-3

[23] Abbas IA. Generalized magneto-thermoelasticity in a nonhomogeneous isotropic hollow cylinder using the finite element method. Archive of Applied Mechanics. 2009;**79**:41-50. DOI: 10.1007/s00419-008-0206-9

[24] Abd-Alla AM, Fahmy MA, El-Shahat TM. Magneto-thermo-elastic problem of a rotating non-homogeneous anisotropic solid cylinder. Archive of Applied Mechanics. 2008;**78**:135-148

[25] Fahmy MA. A time-stepping DRBEM for magneto-thermo-viscoelastic interactions in a rotating nonhomogeneous anisotropic solid. International Journal of Applied Mechanics. 2011;**3**:1-24

[26] Fahmy MA. A time-stepping DRBEM for the transient magneto-thermo-visco-elastic stresses in a rotating non-homogeneous anisotropic solid. Engineering Analysis with Boundary Elements. 2012;**36**: 335-345

[27] Fahmy MA. Boundary element modeling and simulation of biothermomechanical behavior in anisotropic laser-induced tissue hyperthermia. Engineering Analysis with Boundary Elements. 2019;**101**: 156-164

[28] Fahmy MA. Boundary element algorithm for modeling and simulation of dual-phase lag bioheat transfer and biomechanics of anisotropic soft tissues. International Journal of Applied Mechanics. 2018;**10**:1850108

[29] Fahmy MAA. New computerized boundary element algorithm for cancer modeling of cardiac anisotropy on the ECG simulation. Asian Journal of Research in Computer Science. 2018;**2**: 1-10

[30] Fahmy MA. Transient magneto-thermoviscoelastic plane waves in a non-homogeneous anisotropic thick strip subjected to a moving heat source. Applied Mathematical Modelling. 2012; **36**:4565-4578

[31] Fahmy MA. Numerical modeling of transient magneto-thermo-viscoelastic waves in a rotating nonhomogeneous anisotropic solid under initial stress. International Journal of Modeling, Simulation and Scientific Computing. 2012;**3**:1250002

[32] Fahmy MA. The effect of rotation and inhomogeneity on the transient magneto-thermoviscoelastic stresses in an anisotropic solid. ASME Journal of Applied Mechanics. 2012;**79**:1015

[33] Fahmy MA. Transient magneto-thermo-viscoelastic stresses in a rotating nonhomogeneous anisotropic solid with and without a moving heat source. Journal of Engineering Physics and Thermophysics. 2012;**85**: 950-958

[34] Fahmy MA. Transient magneto-thermo-elastic stresses in an anisotropic viscoelastic solid with and without

moving heat source. Numerical Heat Transfer, Part A: Applications. 2012;**61**: 547-564

[35] Fahmy MA. Implicit-explicit time integration DRBEM for generalized magneto-thermoelasticity problems of rotating anisotropic viscoelastic functionally graded solids. Engineering Analysis with Boundary Elements. 2013; **37**:107-115

[36] Fahmy MA. Generalized magneto-thermo-viscoelastic problems of rotating functionally graded anisotropic plates by the dual reciprocity boundary element method. Journal of Thermal Stresses. 2013;**36**:1-20

[37] Fahmy MA. A three-dimensional generalized magneto-thermo-viscoelastic problem of a rotating functionally graded anisotropic solids with and without energy dissipation. Numerical Heat Transfer, Part A: Applications. 2013;**63**:713-733

[38] Fahmy MA. A computerized DRBEM model for generalized magneto-thermo-visco-elastic stress waves in functionally graded anisotropic thin film/substrate structures. Latin American Journal of Solids and Struc tures. 2014;**11**:386-409

[39] Fahmy MA. Computerized Boundary Element Solutions for Thermoelastic Problems: Applications to Functionally Graded Anisotropic Structures. Saarbrücken, Germany: LAP Lambert Academic Publishing; 2017

[40] Fahmy MA. Boundary Element Computation of Shape Sensitivity and Optimization: Applications to Functionally Graded Anisotropic Structures. Saarbrücken, Germany: LAP Lambert Academic Publishing; 2017

[41] Fahmy MA. Shape design sensitivity and optimization for two-temperature generalized magneto-thermoelastic problems using time-domain DRBEM. Journal of Thermal Stresses. 2018;**41**: 119-138

[42] Fahmy MA. Shape design sensitivity and optimization of anisotropic functionally graded smart structures using bicubic B-splines DRBEM. Engineering Analysis with Boundary Elements. 2018;**87**:27-35

[43] Fahmy MA. Modeling and optimization of anisotropic viscoelastic porous structures using CQBEM and moving asymptotes algorithm. Arabian Journal for Science and Engineering. 2019;**44**:1671-1684

[44] Fahmy MA. A new LRBFCM-GBEM modeling algorithm for general solution of time fractional order dual phase lag bioheat transfer problems in functionally graded tissues. Numerical Heat Transfer, Part A: Applications. 2019;**75**:616-626

[45] Fahmy MA. Design optimization for a simulation of rotating anisotropic viscoelastic porous structures using time-domain OQBEM. Mathematics and Computers in Simulation. 2019;**66**: 193-205

[46] Fahmy MA. A new boundary element strategy for modeling and simulation of three temperatures nonlinear generalized micropolar-magneto-thermoelastic wave propagation problems in FGA structures. Engineering Analysis with Boundary Elements. 2019;**108**:192-200

[47] Aniskin A, Orobey VF, Kolomiets LV, Lymarenko AM. Calculation of displacements and stresses in cylindrical shells by the boundary elements method. Technical Journal. 2018;**12**:196-203

[48] Fahmy MA. DRBEM sensitivity analysis and shape optimization of rotating magneto-thermo-viscoelastic FGA structures using DRBEM-GSS and DRBEM-NGGP algorithms. In:

Advances in Mathematics and Computer Science. Vol. 1. London, United Kingdom: Book Publisher International; 2019. pp. 83-104

[49] Fahmy MA. The effect of anisotropy on the structure optimization using BEM-GSS and BEM-NGGP algorithms. In: Advances in Mathematics and Computer Science. Vol. 1. London, United Kingdom: Book Publisher International; 2019. pp. 137-156

[50] Fahmy MA, Al-Harbi SM, Al-Harbi BH, Sibih AM. A computerized boundary element algorithm for modeling and optimization of complex magneto-thermoelastic problems in MFGA structures. In: Advances in Applied Science and Technology. Vol. 2. London, United Kingdom: Book Publisher International; 2019. pp. 139-152

[51] Fahmy MA. Boundary element model for nonlinear fractional-order heat transfer in magneto-thermoelastic FGA structures involving three temperatures. In: Mechanics of Functionally Graded Materials and Structures. London, United Kingdom: IntechOpen; 2019